Cancer Letters 378 (2016) 38–50

Contents lists available at ScienceDirect

Cancer Letters

journal homepage: www.elsevier.com/locate/canlet

Original Articles

Phosphodiesterase 5/protein kinase G signal governs stemness of prostate cancer stem cells through Hippo pathway

Naihua Liu [a], Liu Mei [a], Xueying Fan [a], Chao Tang [a], Xing Ji [a], Xinhua Hu [a], Wei Shi [a], Yu Qian [b], Musaddique Hussain [a], Junsong Wu [c], Chaojun Wang [c], Shaoqiang Lin [d], Ximei Wu [a,e,*]

[a] Department of Pharmacology, School of Medicine, Zhejiang University, Hangzhou, China
[b] Shaoxing People's Hospital of Zhejiang University, Hangzhou, China
[c] The First Affiliated Hospital of Zhejiang University, Hangzhou, China
[d] The First Affiliated Hospital of Jinan University, Guangzhou, China
[e] Program of Molecular and Cellular Biology, School of Medicine, Zhejiang University, Hangzhou, China

ARTICLE INFO

Article history:
Received 3 February 2016
Accepted 8 May 2016

Keywords:
Cancer stem cells
Stemness
PDE5
Hippo pathway
TAZ

ABSTRACT

Cancer stem cells (CSC) are critical for initiation, metastasis, and relapse of cancers, however, the underlying mechanism governing stemness of CSC remains unknown. Herein, we have investigated the roles of phosphodiesterase 5 (PDE5) in stemness of prostate cancer cells. Both PDE5 and WW domain-containing transcription regulator protein-1 (TAZ), a core effector of Hippo pathway, are highly expressed in the PC3-derived cancer stem cells (PCSC). Either TAZ knockdown or inhibition of PDE5 activity attenuated colony formation, altered expression patterns of stem cell markers, and enhanced cisplatin cytotoxicity, resulting in attenuation of stemness in PCSC. In addition, inhibition of PDE5 activity by its specific inhibitors activates cGMP-dependent protein kinase G (PKG), which in turn induces MST/LATS kinases, resulting in cytosolic degradation of TAZ and activation of Hippo pathway. Accordingly, knockdown of TAZ almost completely abolished PDE5 inhibitor-induced attenuation in stemness in cultured PCSC, whereas knockdown of TAZ not only abolished PDE5 inhibitor-induced attenuation in stemness but also facilitated PDE5 inhibitor-induced trans-differentiation in PCSC xenografts. Together, the present study has uncovered that PDE/cGMP/PKG signal targets to Hippo/TAZ pathway in maintaining stemness of PCSC, and suggested that PDE5 inhibitors in combination with chemotherapeutic agents could effectively prevent initiation, metastasis, and relapse of prostate cancer.

Introduction

Prostate cancer is a frequently diagnosed and relapsed male malignancy. Recently, a tiny population of prostate cancer cells characterized by slow growth, self-renewing and asymmetric division, had been isolated and defined as prostatic cancer stem cells (PCSC) [1,2]. Like other cancer stem cells, PCSC are the emerging interpretation for prostate cancer initiation, metastasis, relapse and chemoresistance [3–5], however, the molecular mechanisms governing the stemness and differentiation of PCSC remain elusive.

Hippo signaling pathway has conserved roles in metazoans ranging from Drosophila to humans [6,7]. In mammals, cell–cell junctions and apicobasal polarity are involved in upstream activation of Hippo cascade, and the core to Hippo pathway is a kinase cascade, wherein Ste20-like kinases, Mst1/2, phosphorylate and activate the nuclear dbf2-related family kinases, Lats1/2. Lats1/2 kinases in turn phosphorylate two major downstream effectors, Yes-associated protein (YAP) and transcriptional co-activator with PDZ-binding motif (TAZ), resulting in their ubiquitination and proteolysis [8,9]. On the country, silence of Hippo signaling enhances nuclear location of YAP and TAZ, which subsequently bind to Sd homologs TEAD1/4 and other transcription factors to promote transcription of target genes, such as connective tissue growth factor (ctgf) and cysteine-rich angiogenic inducer 61 (cyr61) [6,7,10]. The Hippo pathway plays crucial roles in not only contact inhibition, organ size control and stem cell maintenance but also cancer stem cell maintenance, and Hippo

Abbreviations: 5'-GMP, guanosine-5'-monophosphate; cGMP, cyclic guanosine monophosphate; CSCs, cancer stem cells; ED, erectile dysfunction; eNOS, endothelial NOS; GC, guanylyl cyclase; iNOS, inducible NOS; LATS, nuclear dbf2-related family kinases or large tumor suppressor kinase; MST, mammalian ste20-like protein kinase; NO, nitric oxide; NOS, nitric oxide synthase; PCSC, prostate cancer stem cells; PDE5, phosphodiesterase 5; PKG, cGMP-dependent protein kinase; PSA, prostate specific antigen; sGC, soluble guanylyl cyclases; TAZ, WW domain-containing transcription regulator protein 1; TEADs, TEA domain family members; YAP, Yes associated protein.

* Corresponding author. Tel: +86 571 8898 1121; fax: +86 571 8898 1121.
E-mail address: xiwu@zju.edu.cn (X. Wu).

http://dx.doi.org/10.1016/j.canlet.2016.05.010
0304-3835/

pathway disruption is closely associated with poor outcome in a variety of malignancies [7,11]. TAZ is elevated in high-grade breast cancer and contributes to breast cancer stem cell self-renewal [12]. YAP but not TAZ up-regulates CD90, a hepatocellular carcinoma-specific cancer stem cell marker, resulting in tumorigenesis and chemoresistance in hepatocellular carcinoma [13]. In addition, YAP is activated by ETS-related gene (ERG), and contributes to development of age-related prostate tumors [14], whereas aberrantly overexpressed YAP sufficiently transforms LNCaP prostate cancer cells to an androgen-insensitive state responsible for castration resistance [15]. However, whether Hippo tumor suppressor pathway is correlated with stemness and differentiation of PCSC remains elusive.

Cyclic guanine monophosphate (cGMP) activated by soluble guanylyl cyclases and degraded by cyclic nucleotide phosphodiesterases (PDEs) mediates biological signaling by nitric oxide (NO). cGMP binds and activates cGMP-dependent protein kinases (PKGs), which phosphorylate serine and threonine residues on many cellular proteins, resulting in changes in their activity, subcellular localization or regulatory features [16,17]. Current therapies targeting the nitric oxide (NO)-signaling pathway include nitrovasodilators, such as nitroglycerin and sodium nitroprusside, and PDE5 inhibitors, such as sildenafil, vardenafil, and tadalafil for treatment of a number of vascular diseases including angina pectoris, erectile dysfunction, and pulmonary hypertension [18,19]. Recently, several studies have hinted at the possible effect of NO/cGMP on stem cell differentiation [20,21]. NO synthetase (NOS) inhibitors increase the number of bone marrow derived hematopoietic stem cells, whereas NO signaling promotes differentiation of embryonic stem cells into myocardial cells [22]. Moreover, PDE5 inhibition improves adipose-derived stem cells survival, and the combination of PDE5 inhibition and adipose-derived stem cells benefits to the rehabilitation of myocardial infarction [23]. Finally, because elevated PDE5 expression has been reported in multiple human carcinomas and in many carcinoma cell lines [24,25] and its elevation occurs with increasing tumor grade and stage, PDE5 has been suggested to be involved in tumor initiation and progression [26]. Accordingly, PDE5 inhibitors are believed to be potent anticancer drugs with a novel mechanism of actions including enhancing the apoptosis, anti-proliferation, efficacy of chemotherapy and attenuating chemoresistance and multi-drug resistance [27,28]. However, whether PDE5 and its inhibitors contribute to the stemness and differentiation of PCSC remains largely elusive.

In the present study, we have investigated the underlying mechanisms by which PDE5/cGMP/PKG signal governs stemness and differentiation of PCSC. We have found that inhibition of PDE5 enhances the differentiation and attenuates the stemness of PCSC through activation of Hippo/TAZ signaling pathway.

Materials and methods

Cell lines and culture

Prostatic carcinoma cell lines, including PC3 and DU145 cells were purchased from ATCC (Manassas, VA). PC3 cells were maintained in Dulbecco's Modified Eagle Medium: Nutrient Mixture F-12 (DMEM/F-12) containing 1 × GlutaMAX™, 7% fetal bovine serum (Life Technologies, Inc., Carlsbad, CA), 100 U/ml penicillin, and 100 μg/ml streptomycin. DU145 cells were maintained in RPMI-1640, 7% fetal bovine serum, 100 U/ml penicillin, and 100 μg/ml streptomycin. All cell lines were incubated at 37 °C with 5% CO2.

Isolation of PC3-derived PCSC by limiting dilution

The PC3 derived prostate cancer stem cells were isolated and purified as previously described [1,2]. In belief, PC3 cells were harvested and washed with FBS-free DMEM/F-12 medium twice, then re-suspended in DMEM/F-12 medium containing 5% FBS and 1 × GlutaMAX™ (Invitrogen) to generate a single-cell suspension with a density of 10 cells/ml. 100 μl/well single-cell suspension was plated into 96-well plates. After 24 h, wells containing only a single cell were marked and further maintained in DMEM/F-12 medium containing 5% FBS and 1 × GlutaMAX™. After 3–4 weeks, cells grew to confluence and the culture medium was replaced with PC3 cell growth medium, then, each clone was expanded and subjected to identification of stem cell-like properties.

Western blot assays

Cells were seeded to 6-well plate at 70–80% confluence, and cultured for 48 h, then treated with or without indicated concentrations of vardenafil HCl trihydrate (Selleckchem, Houston, TX) for further indicated time for western blot. Protein extracts from cells or tumor samples were prepared in whole cell lysis buffer (50 mM HEPES, 150 mM NaCl, 1 mM EGTA, 10 mM sodium pyrophosphate, 1.5 mM $MgCl_2$, 100 mM sodium fluoride, 10% glycerol, and 1% TritonX-100) containing an inhibitor mixture (1 mM phenylmethysulfonyl fluoride, 10 μg/ml aprotinin, and 1 mM sodium orthovamadate). Protein concentrations were determined using a standard Bradford assay, and 50 μg of total protein was subjected to SDS-PAGE followed by a transfer onto 0.45 μm PVDF membranes (Millipore, Bedford, MA). Membranes were incubated overnight at 4 °C with primary antibodies. Antibodies against p-TAZ, TAZ, YAP, PKG2, Nanog, Lamin B, Glyceraldehyde-3-phosphate dehydrogenase (GAPDH) and β-actin were from Santa Cruz Biotechnology (Santa Cruz, CA), antibodies against p-MST, p-LATS, p-YAP, MST1, and LATS1 were from Cell Signaling (Danvers, MA), antibodies against PDE5a and PKG1 were obtained from Abcam (Cambridge, UK), antibodies against Sox2 and CTGF were from BBI Life Sciences Corporation (Shanghai, China), and antibodies against myc-tag, HA-tag and flag-tag were from TransGen Biotech (Beijing, China). The IRDye 680 and 800 second antibodies were purchased from LI-COR Bioscience (Lincoln, Nebraska). The immunoreactive signals were visualized with Odyssey Infrared Imaging System (LI-COR, Lincoln, NE), and GAPDH or β-actin was used as internal standards. ImageJ software from National Institutes of Health (http://rsb.info.nih.gov/ij/download.html) was used to quantify the immunoreactive bands, and the mean intensity of the first band was set to 1.

RNA isolation and quantitative RT-PCR

Cells were seeded using a 6-well plate and at 70–80% confluence, cultured for 48 h, and then treated with or without indicated concentrations of vardenafil for a further 6 h for RT-qPCR. Total RNA was isolated by using Trizol reagent (Takara Biotechnology Co., Ltd., Dalian, China) according to the manufacturer's instructions. 1 μg total RNA in a volume of 20 μl was reversely transcribed by using SuperScript III reagent (Life Technologies). After termination of cDNA synthesis, each reaction mixture was diluted with 80 μl Tris-EDTA buffer. Messenger RNA levels of target genes were determined by quantitative RT-PCR as previously described [29]. The relative amounts of the mRNA levels of the target genes were normalized to the glyceraldehyde-3-phosphate dehydrogenase (GAPDH) and β-actin levels, respectively, and the relative difference in mRNA levels was calculated by $2^{-\Delta\Delta Ct}$ method.

Cell counting kit-8 assays

Cells were seeded into 96-well plates at 1000 cells/well, and cultured for 8 days. Cellular vitality was measured every two days by cell counting kit-8 (Beyotime, Shanghai, China) as per manufacturer's instructions. In chemoresistance experiments, cells were seeded into 96-well plates at 5000 cells/well, after culture for 24 hours, cells were treated with indicated concentrations of Cisplatin (Sigma, St. Louis, MO) for a further 48 hours, and then cellular vitality was measured by cell counting kit-8. The cytotoxicity (%) = [1 – (OD from tested cells)/OD from control cells]*100%.

Mammosphere formation assays

Mammosphere formation assays were performed as previously described [2]. In belief, cells were harvested and washed with FBS-free DMEM/F-12 medium twice, then re-suspended in FBS-free DMEM/F-12 medium containing 1 × B27 (Invitrogen), 20 ng/ml human bFGF (PeproTech, Rocky Hill, NJ), 20 ng/ml human EGF (PeproTech), and 3 μg/ml insulin (Sigma, St. Louis, MO). After that, single cells were seeded into 6-well Ultra–Low Attachment plates (Corning, NY) at a density of either 5×10^4 or 1×10^5 cells/well and half volume of medium was carefully changed every 2 days. After two weeks, spheres were captured by Olympus fluorescence microscope.

Clone formation assays

Clone formation assays were performed as previously described [2]. In belief, cells were harvested and washed twice, then re-suspended in 5% FBS-free DMEM/F-12 medium containing 1 × GlutaMAX™; single cells were plated in 6-well plates at a density of 1000. The medium containing vehicle or vardenafil was carefully changed every 2 days for two weeks, then cells were washed twice and stained with crystal violet. Clones of each well were captured and subsequently analyzed by ClonCounter software [30].

Fluorescence-activated cell sorting

Cells were re-suspended at a density of 1×10^6 cells/ml, and then intracellular NO were labeled by 5 μM 3-Amino,4-aminomethyl-2',7'-difluorescein, diacetate

(DAF-FM DA, Beyotime) for 20 min at 37 °C, and DAF-FM DA dilution buffer served as a negative control. After washed for three times with PBS, cells were re-suspended in PBS containing 1%FBS, and then passed through a 40 μm cell strainer (FALCON, Corning, USA), all single-cell suspensions were collected and sorted immediately by BD FACSAria II cell sorter (BD, USA). The sample was defined with forward scatter channel and side scatter channel plot, then the detector was set up with negative control and DAF-FM DA staining (excitation at 490 nm and emission at 515 nm); NO^{low} and NO^{high} subsets were sorted and collected for subsequent analyses.

Isolation of cytosolic and nuclear fractions, immunoprecipitations, and immunofluorescence

Cells were seeded to 100 mm dish at 70–80% confluence, and cultured for 48 h, then treated with or without indicated concentrations of vardenafil for a further 12 h for isolation of cytosolic and nuclear fractions. Cytosolic and nuclear fractions were prepared by using NE-PER Nuclear and Cytoplasmic Extraction Reagents (Thermo Scientific, Waltham, MA) as the manufacturer's instruction. Then, the protein samples were subjected to western blot assays. Immunoprecipitations were performed as previously described [17], cells were seeded to 100 mm dish at 70–80% confluence, and cultured for overnight, then after transfected with indicated vectors and cultured for 36 h, then treated with or without indicated concentrations of vardenafil for a further 1 h. Cells were harvested and lysated in immunoprecipitation lysis buffer (Beyotime), and 1 ml of 500 μg total cellular protein was incubated with 2 μg primary monoclonal antibody overnight at 4 °C. Protein A/G PLUS-Agarose was added as per manufacturers' instruction (Santa Cruz) and the samples were rotated overnight at 4 °C, pellets were harvested and washed as per manufacturers' instruction. After boiled, samples were subjected to western blot assays. Immunofluorescence was performed as previously described [17], cells were seeded to 20 mm cell culture cover slip at 70–80% confluence, and cultured for 48 h, then treated with or without indicated concentrations of vardenafil for a further 12 h, and then cells were fixed in 4% PFA/PBS, neutralized by NH4Cl at 50 mM, and permeabilized with 0.1% Triton X100/PBS. After blocked with 5%BSA/5%non-fat milk/PBST, cells were incubated with TAZ antibody (1:50) for 1 hour followed by washing and further incubation with Alexa Fluor® 647 goat anti-rabbit antibody (1:200, Invitrogen). After being washed, cells were counterstained with 4',6-diamidino-2-phenylindole (DAPI). Samples were captured by Olympus confocal fluorescence microscope.

Transient transfection and dual-luciferase assay

Transient transfections were performed by using Attractene Transfection Reagent (QIAGEN, Hilden, Germany) as per manufacturer's instruction. Briefly, cells were seeded in 24-well plate overnight to reach 70–80% confluence before transfection. 1.5 μl Attractene Transfection Reagent, 0.1 μg TAZ plasmid, 0.2 μg TEAD4 luciferase reporter plasmid, and 0.1 μg pRL-null expressing Renilla luciferase were used for transfection for 6 hours. Media were changed to fresh normal growth medium and cultured for 42 h, and after treating with or without indicated concentrations of vardenafil for a further 12 hours, the dual-luciferase assay was performed as per manufacturer's instruction (Promega, Madison, WI).

Establishment of scramble- and TAZ-shRNA-expressing PC3 cells and PCSC

Three pairs of specific shRNA sequences which target the three sites of TAZ encoding sequences and one pair of scramble shRNA sequence were cloned into lentivarial shRNA-expressing vector, pSicoR-GFP. Scramble- and TAZ-shRNA-expressing lentiviruses were prepared by Hanbio Company (Shanghai, China), and lentiviruses with titer more than 1×10^8 PFU/ml were used in the experiments. Stably scramble- and TAZ-shRNA-expressing PC3 cells and PCSC were generated by combination of three TAZ RNAi sequences lentiviral supernatants. Cells were infected with lentiviruses expressing scramble- and TAZ-shRNA and selected in the growth medium containing G418 (600 μg/ml; Sigma). After that, the highly GFP-expressing clones were expanded and subjected to determining the efficacy of TAZ knockdown.

Mouse models bearing PC3 cells or PCSC xenografts

Mouse models bearing PC3 cells or PCSC xenografts were generated as follows. Scramble-, TAZ-shRNA-expressing PC3 cells or PCSC in PBS at a density of 1×10^7 cells/ml, were subcutaneously inoculate the cells (0.1 ml) into left armpit of adult nude mice (SLAC Laboratory Animal Co., Ltd., Shanghai, China). Each group had 10 mice for injection. 15 days after inoculation, xenografts started to emerge, and the body weights were recorded every three days within 40 days. For scramble- and TAZ-expressing PC3 cells or PCSC xenocrafts, mice were randomized to intragastrically receive either vardenafil at 40 mg/kg/day or vehicle from day 15. The volume of xenograft was calculated by the formula $(V) = (a + b) \times (a) \times (b) \times (0.2618)$, *V: xenograft volume; a: short diameter; b: long diameter. Mice were sacrificed on day 40 and the xenografts were harvested for Ki67 and TUNEL staining, preparation of protein lysates and isolation of total RNA. All mice were housed at Zhejiang University Animal Care Facility according to the institutional guidelines for laboratory animals and the protocol was approved by the Zhejiang University Institutional Animal Care and Use Committee.

Immunohistochemistry analysis for ki67 and TUNEL assay

Xenografts were subjected to preparation of paraffin-embedded tumor tissue sections, and the sections were processed for immunohistochemistry analysis for Ki67 by Ki67 Cell Proliferation Kit (Sangon Biotech, Shanghai, China) and TUNEL staining by One-Step TUNEL assay (Beyotime). The images were captured by Olympus fluorescence microscope, and further analyzed by ImageJ 1.48v software.

Statistical analysis

Numerical data were expressed as mean ± S.D., and statistical analyses were performed by one-way ANOVA and Tukey–Kramer multiple comparison test (GraphPad Software Inc., La Jolla, CA). $p < 0.05$ and $p < 0.01$ were considered to be statistically significant. Experiments were independently triplicated, and results were qualitatively identical. Representative experiments are shown.

Results

Isolation and characteristics of PCSC from PC3 cells

To gain quantitative information about the expression of main components of PDE5/cGMP/PKG and Hippo/TAZ signaling pathways in PC3 and DU145 cells, we performed western blot and quantitative RT-PCR assays. PDE5a protein levels were 1.0-fold higher in PC3 cells than in DU145 cells, whereas TAZ protein levels were 9.0-fold higher in PC3 cells than in DU145 cells (Fig. 1A). *β-catenin* mRNA was almost evenly expressed in PC3 and DU145 cells, whereas the mRNAs of *pde5a*, *pkg1*, *pkg2*, and *taz* were expressed significantly more in PC3 cells than in DU145 cells (Fig. 1B). The higher expression of both PDE5a and TAZ in PC3 cells than in DU145 cells rationally prompts us to isolate and characterize the PCSC from PC3 cells. Quantitative RT-PCR assays were performed to investigate the expression pattern of PCSC's markers including *cd24*, *lcp1*, and *fam65b*. The parent PC3 cells expressed 9.0- and 200-fold more *cd24* and l*cp*1 mRNA but 3.8-fold less *fam65b* mRNA than PCSC (Fig. 1C). Moreover, CCK-8 assays were performed to determine the proliferation of PC3 cells and PCSC in the presence or absence of chemotherapeutic agent, cisplatin (DDP). Within 8 days post-seeding, the parent PC3 cells proliferated more rapidly than PCSC, and on day 8, the proliferation rate of PC3 cells was approximately 3.0-fold higher than that of PCSC (Fig. 1D). DDP treatments ranging from 0 μM to 400 μM dose-dependently induced the cytotoxicity to both PC3 cells and PCSC, however, PC3 cells were more sensitive to DDP treatment than PCSC, and DDP at 100 μM led to 1.0-fold more cytotoxicity to PC3 cells than to PCSC (Fig. 1E). Finally, mammosphere formation assays were performed to evaluate cellular transformation in PC3 cells and PCSC. PCSC formed approximately 5.0-fold more mammospheres than PC3 cells at a density of 0.5×10^5 cells/well, whereas PCSC formed approximately 4.0-fold more mammospheres than PC3 cells at a density of 1.0×10^5 cells/well (Fig. 1F). Thus, prostate cancer cells express the main components of both PDE5/cGMP/PKG and Hippo/TAZ pathways, and PC3 cells-derived PCSC possess stem cell-like characteristics.

Requirement of TAZ but not YAP in maintaining stemness of PCSC

To investigate the potential roles of Hippo signaling in maintaining stemness of PCSC, we determined the protein levels of TAZ and YAP and knocked down the expression of TAZ in PC3 cells and PCSC. The mRNA levels of both *taz* and *yap* exhibited no significant difference between in PC3 cells and in PCSC (Fig. S1A). Though YAP protein levels in PCSC were similar to those in PC3 cells, the protein levels of TAZ and stem cell markers including Nanog and Sox2 in PCSC were approximately 2.9-, 3.5-, and 1.7-fold higher than those in PC3 cells, respectively (Fig. 2A). To determine whether high expression of TAZ contributes to maintaining the stemness of PCSC, we next knocked down the TAZ by TAZ-shRNA-expressing lentiviruses. TAZ-shRNA reduced the TAZ protein levels by 40% and

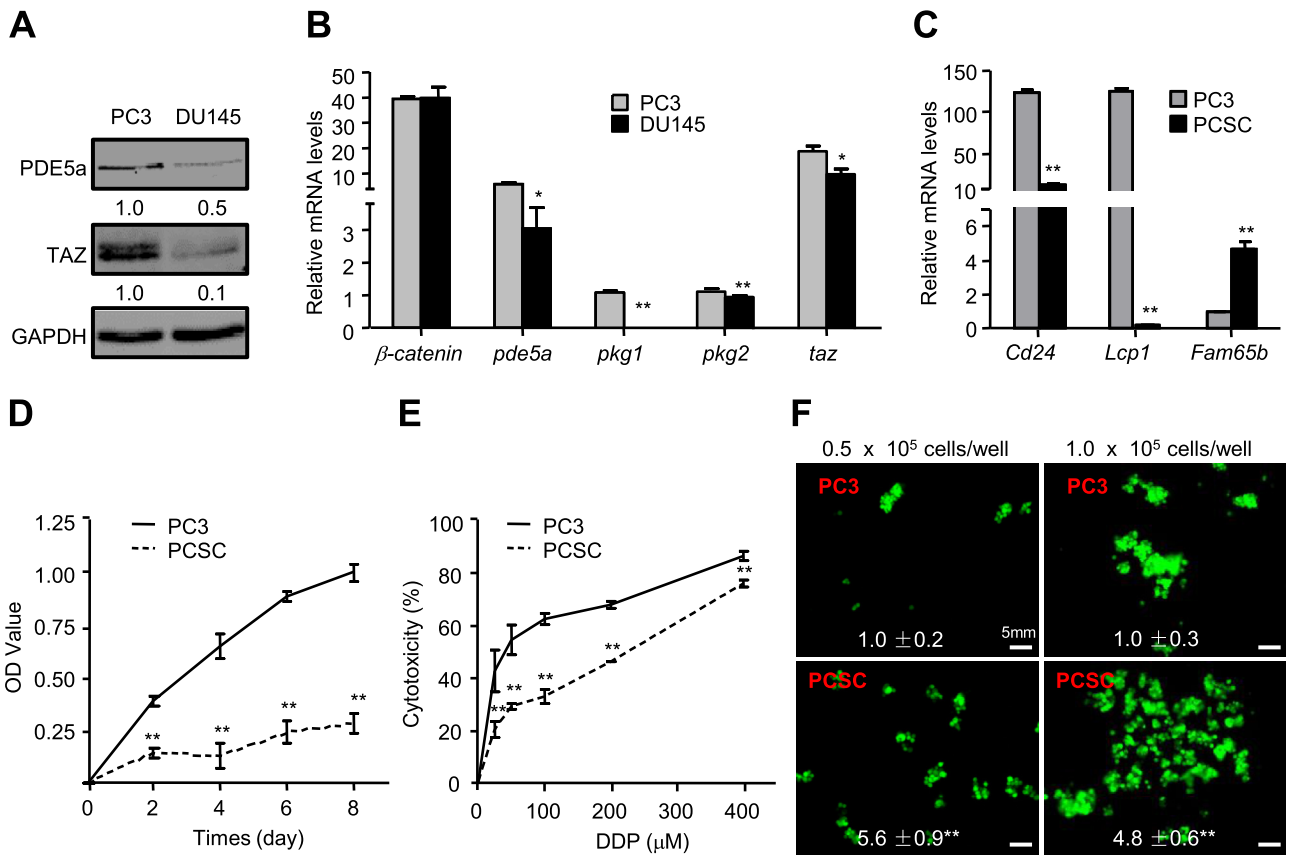

Fig. 1. Isolation and characteristics of PC3-derived PCSC.
(A) Immunoblot analysis for the indicated proteins in PC3 and DU145 cells. (B) Quantitative RT-PCR assays for mRNA levels of indicated genes in PC3 and DU145 cells. (C) Quantitative RT-PCR assays for mRNA levels of indicated genes in PC3 cells and PCSC. (D) CCK8 assays for PC3 cells and PCSC cultured in medium contained 2% FBS for indicated times. (E) Cytotoxicity to PC3 cells and PCSC treated with indicated concentrations of DDP for 48 hours. (F) Mammosphere formation assays in PC3 cells and PCSC lentiviral expressing GFP. $^{**}p < 0.01$, $^{*}p < 0.05$ versus PC3 cells.

80% in PC3 cells and PCSC, respectively, and significantly decreased the Nanog protein by 20% and 52% in PC3 and PCSC, respectively (Fig. 2B). Though TAZ knockdown significantly reduced *fam65b* mRNA levels in both PC3 cells and PCSC, TAZ knockdown significantly increased *cd24* mRNA levels only in PCSC but not in PC3 cells (Fig. 2C). Moreover, TAZ knockdown significantly decreased the colony formations by 42% and 72% in PC3 cells and PCSCs, respectively (Fig. 2D). Remarkably, TAZ knockdown slightly increased the cytotoxicity to PCSC but not to PC3 cells, and TAZ knockdown unaffected DDP-induced cytotoxicity to PC3 cells but significantly potentiated DDP-induced cytotoxicity to PCSC by approximately 5.0-fold (Fig. 2E). Taken together, these data suggest that TAZ but not YAP is required for the stemness of PC3 cells-derived PCSC.

Requirement of PDE5/cGMP/PKG signaling in maintaining stemness of PCSC

Next, we determined the expression of key components of PDE5/cGMP/PKG signaling pathway and investigated their roles in stemness of PCSC. PCSC expressed 2.8-fold more PDE5a than PC3 cells, whereas PCSC expressed 60% less PKG1 and 70% less PKG2 than PC3 cells, respectively (Fig. 3A). In addition, except for *pde5a* mRNA that was expressed more in PCSC than in PC3 cells, mRNAs of inducible NOS (*iNOS*), endothelial NOS (*eNOS*), *pkg1*, and *pkg2* in PC3 cells were expressed significantly more in PC3 cells than in PCSC cells (Fig. 3B). Consistent with the mRNA expression of *iNOS* and *eNOS*, endogenous NO levels in PCSC were approximately 42% less than those in PC3 cells (Fig. 3C, Fig. S1B). Moreover, inhibition of PDE5 activity by a specific inhibitor, vardenafil (Vard.) ranging from 0 μM to 100 μM dose-dependently reduced *fam65b* mRNA levels but increased *cd24* mRNA levels; vardenafil at 100 μM reduced *fam65b* mRNA levels by 60% but increased *Cd24* mRNA levels by 40% in PCSC (Fig. 3D). Likewise, vardenafil ranging from 0 μM to 100 μM dose-dependently suppressed colony formation in both PC3 cells and PCSC; vardenafil at 100 μM reduced colony formation by 90% and 95% in PC3 cells and PCSC, respectively (Fig. 3E, F). Moreover, vardenafil ranging from 0 μM to 50 μM dose-dependently attenuated TAZ as well as Nanog protein levels in PCSC and vardenafil at 50 μM reduced TAZ and Nanog protein levels by 70% and 80%, respectively (Fig. 3G). Finally, DDP ranging from 0 μM to 50 μM dose-dependently induced cytotoxicity to PCSC, though vardenafil (50 μM) alone exhibited no marked cytotoxicity to PCSC; vardenafil at 50 μM synergistically potentiated cytotoxicity to PCSC in response to DDP at either 25 μM or 50 μM (Fig. 3H). Taken together, these data suggest that the main components of PDE5/cGMP/PKG signaling pathway are expressed in both PC3 cells and PCSC, and PDE5/cGMP/PKG signaling is essential for stemness of PCSC.

PDE5/cGMP/PKG targeting to Hippo/TAZ pathway

Next, we investigated the effects of PDE5/cGMP/PKG signaling module on Hippo/TAZ pathway. PC3 cells with high endogenous NO levels expressed 40% less TAZ than PC3 cells with low endogenous NO levels (Fig. 4A, Fig. S1C). Likewise, inhibition of PDE5 activity by either vardenafil or tardalafil dose-dependently attenuated TAZ

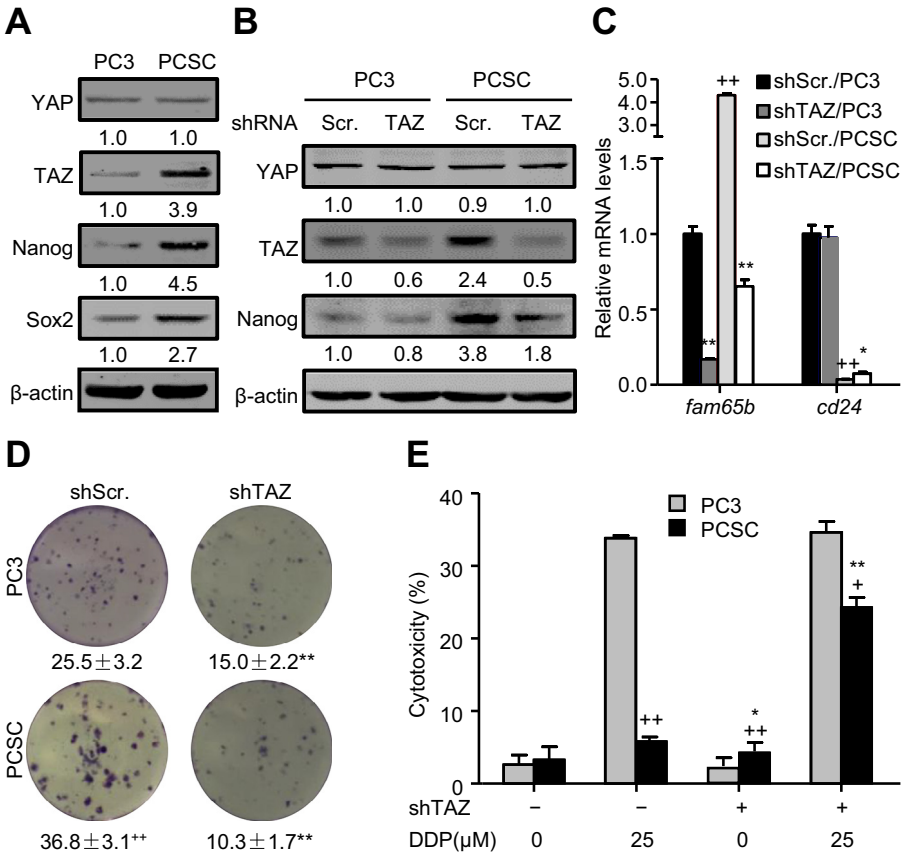

Fig. 2. TAZ is required for stemness of PCSC. (A) Immunoblot analysis for the indicated proteins in parent PC3 cells and PCSCs. (B) Parent PC3 cells and PCSCs were infected by scramble (Scr.)- and TAZ-shRNA expressing lentiviruses, respectively, then immunoblot analysis was performed for the indicated proteins. (C) mRNA levels of stem cell markers in PC3 and PCSC infected with or without scramble (Scr.)- and TAZ-shRNA expressing lentiviruses. (D) Colony formation analysis for the indicated cells. (E) Quantification of colony formation from (d). $^{**}p < 0.01$, $^{*}p < 0.05$ versus shScr.-expressing PC3 cells; $^{++}p < 0.01$, $^{+}p < 0.05$ versus shScr.-expressing PCSC.

protein levels, and vardenafil and tardalafil both at 100 μM decreased TAZ levels by 80% and 90%, respectively (Fig. 4B). Similarly, activation of PKG by 8-Br-cGMP ranging from 0 μM to 100 μM dose-dependently attenuated TAZ levels and 8-Br-cGMP at 100 μM decreased TAZ protein levels by 70% (Fig. 4C). To further confirm the effects of PKG on TAZ levels, cells were transfected with PKG1 siRNA which knocked down the PKG1 protein by 40% in either the presence or absence of vardenafil at 50 μM. Though PKG1 siRNA alone increased TAZ protein levels by 1.3-fold and unaffected the YAP protein levels, PKG1 siRNA reversed vardenafil-negated TAZ levels by 2.0-fold (Fig. 4D). Then, the subcellular localization of TAZ was examined in PC3 cells followed by the treatment with vardenafil ranging from 0 μM to 100 μM. Vardenafil dose-dependently reduced TAZ levels not only in cytoplasmic fractions but also in nuclear factions and vardenafil at 100 μM reduced the cytoplasmic and nuclear fractions of TAZ by both 50% (Fig. 4E). Consistently, immunofluorescent staining for TAZ distribution indicated that vardenafil and tardalafil both at 50 μM markedly recued both cytoslic and nuclear TAZ-derived fluorescent signals (Fig. 4F). To further confirm that activation of cGMP/PKG signaling module inhibits Hippo/TAZ signaling, we performed TEAD4 luciferase assays and quantitative RT-PCR. Vardenafil dose-dependently attenuated TEAD4 luciferase activities in both PC3 cells and DU145 cells, and vardenafil at 100 μM decreased the TEAD4 luciferase activities by 48% and 70% in PC3 and DU145 cells, respectively (Fig. S1D, E). Moreover, vardenafil at 50 μM reduced the TEAD4 luciferase activity by 70% and TAZ overexpression induced TEAD4 luciferase activity by 60%, however, vardenafil reduced TAZ-induced TEAD4 luciferase activity by 90% (Fig. 4G). Likewise, vardenafil dose-dependently decreased the mRNA levels of Hippo/TAZ pathway target genes including *ctgf* and *cyr61* while vardenafil at 100 μM reduced these mRNA levels by 80% and 75%, respectively (Fig. 4H). Conversely, inhibition of PKG activity by a specific inhibitor, KT5823, dose-dependently induced the TEAD4 luciferase activity and TAZ protein levels as well; KT5823 at 2 μM induced TEAD4 luciferase activity and TAZ protein levels by 4.2- and 3.3-fold, respectively (Fig. 4I). Similarly, KT5823 dose-dependently induced the mRNA levels of *ctgf* and *cyr61*, KT5823 at 2 μM increased these mRNA levels by 60% and 90%, respectively (Fig. 4J). Thus, activation of cGMP/PKG signaling by inhibition of PDE5 reduces TAZ and in turn attenuates TAZ-mediated transcriptional activation of Hippo pathway target genes, whereas inhibition of cGMP/PKG signaling induces TAZ and subsequently potentiates TAZ-mediated transcriptional activation of Hippo pathway target genes.

Mechanism underlying cGMP/PKG-mediated activation of Hippo signaling

Next, we explore the potential mechanism governing cGMP/PKG-mediated activation of Hippo signaling. Treatment of PC3 cells with vardenafil ranging from 0 μM to 100 μM for 1 hour led to dose-dependent and significant increases in phosphorylation of MST, LATS, and TAZ but not YAP, and vardenafil at 50 μM increased phosphorylated MST, LATS, and TAZ by 3.4-, 1.1-, and 5.1-fold, respectively (Fig. 5A). Likewise, treatment of PC3 cells with 50 μM vardenafil within 2 hours caused time-dependent increases in phosphorylation of MST, LATS, and TAZ but not YAP either, and vardenafil treatment for 2 hours increased phosphorylated MST, LATS, and TAZ by 3.5-, 1.2-, and 2.8-fold, respectively (Fig. 5B). Moreover,

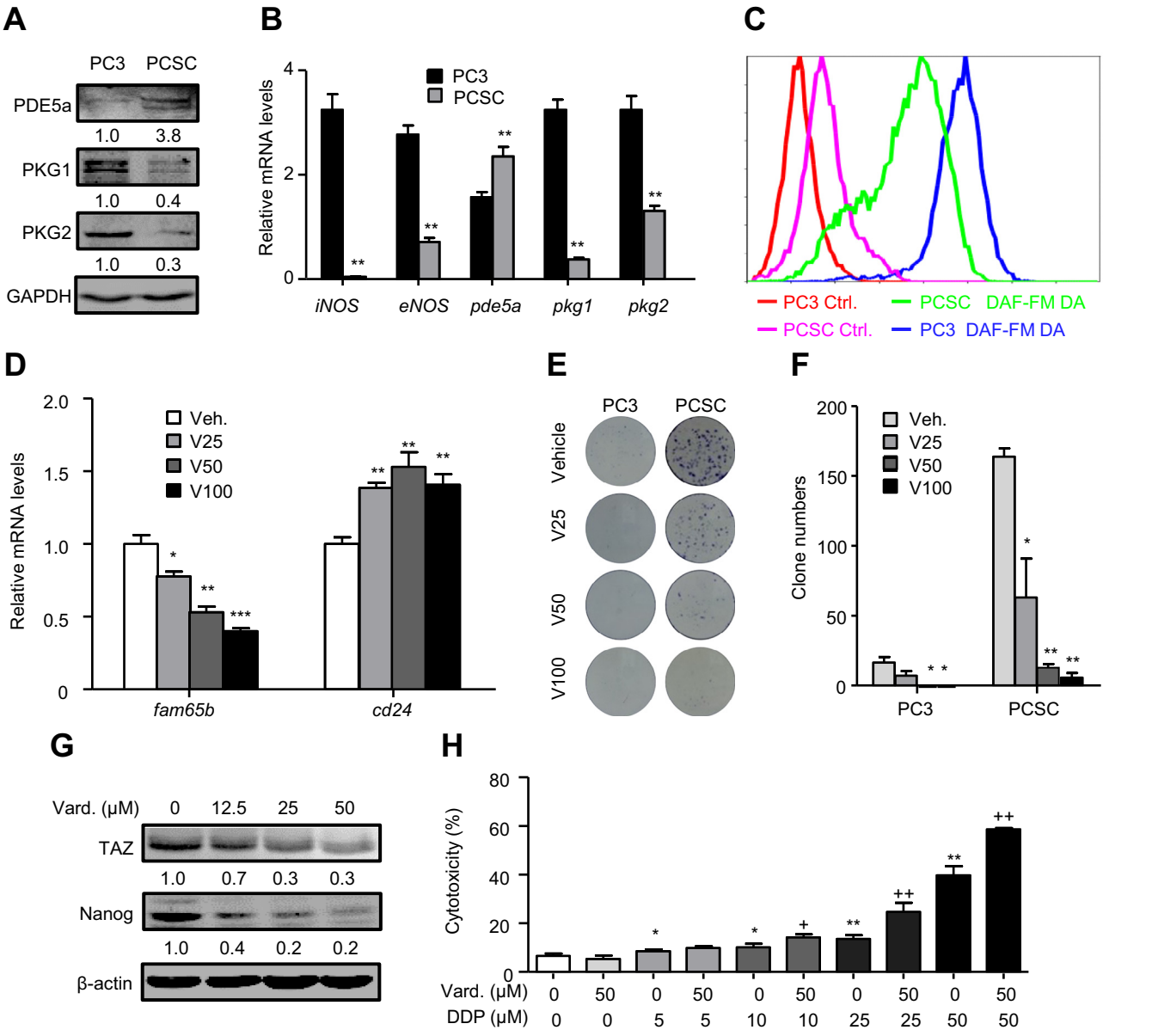

Fig. 3. NO/cGMP/PKG signaling cascade is required for stemness of PCSC. (A) Immunoblot analysis for the indicated proteins in parent PC3 cells and PCSCs. (B) Messenger RNA levels of major components from NO/cGMP/PKG signaling cascade. (C) Endogenous NO in PC3 and PCSC was labeled by DAF-FM DA and analyzed by FACS. (D)The quantitative RT-qPCR analysis for stem cell markers in PC3 and PCSC treated with indicated concentration of vardenafil. (E, F) Colony formation analysis and quantification for PC3 cells and PCSC treated with indicated concentrations of vardenafil. (G) Immunoblot analysis for TAZ and Nanog in PCSC after vardenafil treatments. (H) Cytotoxicity to DDP in PCSC treated with indicated concentrations of vardenafil. $^{**}p < 0.01$, $^{*}p < 0.05$ versus PC3 cells, vardenafil at 0 μM, or DDP at 0 μM; $^{++}p < 0.01$, $^{+}p < 0.05$ versus vardenafil at 0 μM.

overexpression of HA-tagged TAZ (HA-TAZ, WT) induced CTGF protein levels by 5.2-fold, while vardenafil at 50 μM reduced HA-TAZ by 50% and HA-TAZ-induced CTGF levels by 45%, respectively; though point mutation at Serine89 (S89A) led to increases in TAZ levels by 80%, it almost completely abolished vardenafil-negated both TAZ and CTGF levels (Fig. 5C). Consistently, overexpression of wild type of TAZ (WT) increased TEAD4 luciferase activity by 0.6-fold, while overexpression of TAZ mutant resulted in increases in TEAD4 luciferase activity by 2.3-fold (Fig. 5D). Vardenafil at 50 μM reduced WT-induced TEAD4 luciferase activity by 88%, whereas it almost unaffected TAZ mutant-induced TEAD4 luciferase activity (Fig. 5D). Furthermore, in either the presence or absence of vardenafil at 50 μM, protein complexes precipitated with a flag antibody contained abundant myc-tagged PKG1 as well as flag-tagged MST1 as expected (Fig. 5E), while protein complexes precipitated with a HA antibody contained abundant myc-tagged PKG1 as well as HA-tagged TAZ either (Fig. 5F). Finally, in either the presence or absence of vardenafil at 50 μM, protein complexes precipitated with a myc antibody contained abundant MST and TAZ as well as myc-PKG1 as expected, though the protein complex contained little of YAP (Fig. 5G). Taken together, these data suggest that PKG activates Hippo signaling possibly through direct activation of MST kinase.

PDE5/cGMP/PKG signaling targeting to Hippo/TAZ signaling in maintaining stemness of PCSC

To investigate the biological relevance of cGMP/PKG targeting to Hippo/TAZ pathway, we further determined whether cGMP/PKG maintain stemness of PCSC through Hippo/TAZ pathway. In PCSC, vardenafil at 50 μM reduced TAZ and Nanog levels by 60% and 50%,

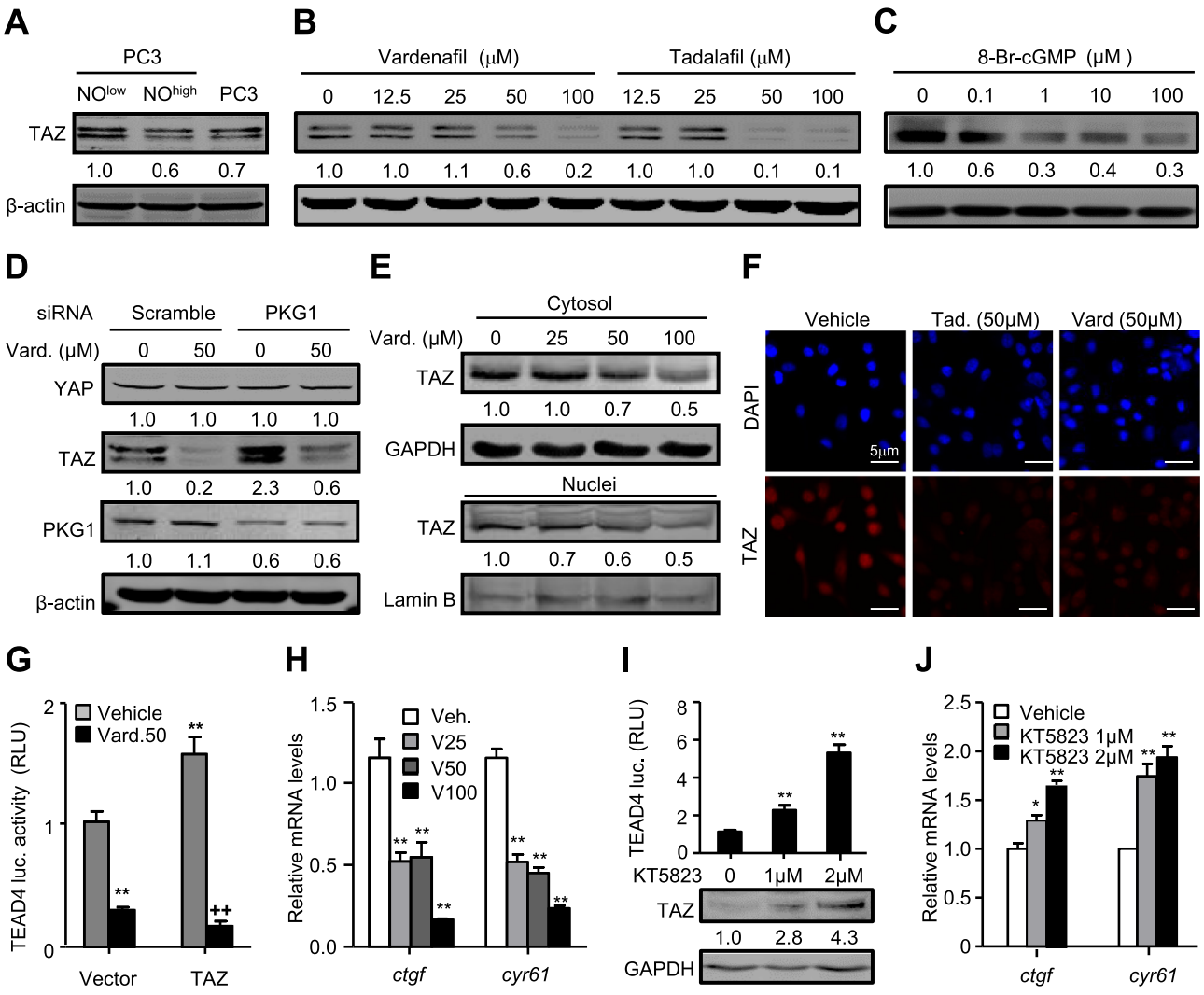

Fig. 4. Inhibition of PDE5 activates Hippo pathway. (A) Immunoblot assay for TAZ in PC3-derived NO^{low} and NO^{high} subsets. (B) Immunoblot assay for TAZ in PC3 cells treated with indicated concentrations of vardenafil or tadalafil for 12 hours. (C) Immunoblot assay for TAZ in PC3 cells treated with indicated concentrations of 8-Br-cGMP for 12 hours. (D) Immunoblot assay for YAP, TAZ, and PKG1 in PC3 cells transfected with PKG1-siRNA, and further treated with or without vardenafil for 12 hours. (E, F) Immunoblot and immunofluorescent assays and for cytosolic and nuclear fractions of TAZ in PC3 cells treated with or without vardenafil or tardalafil for 12 hours. (G) TEAD4 luciferase activity in PC3 cells co-transfected with or without TAZ and treated with or without vardenafil for 36 hours. (H) Quantitative RT-PCR for mRNA levels of *ctgf* and *cyr61* in PC3 cells treated with or without vardenafil for 24 hours. (I) TEAD4 luciferase activity in PC3 cells treated with or without KT5825 for 36 hours. (J) Quantitative RT-PCR for mRNA levels of *ctgf* and *cyr61* in PC3 cells treated with or without KT5825 for 12 hours. $^{*}p < 0.05$, $^{**}p < 0.01$ versus vehicle (Veh.) treatment, $^{++}p < 0.01$ versus TAZ overexpression.

respectively, whereas TAZ shRNA suppressed TAZ and Nanog expression by 50% and 90%, respectively; however, in TAZ-shRNA-expressing PCSC, vardenafil at 50 μM did not reduce Nanog expression any more (Fig. 6A). Moreover, vardenafil at 50 μM reduced the colony formation by 90%, and TAZ shRNA decreased colony formation by 95%; however, in TAZ-shRNA-expressing PCSC, vardenafil at 50 μM did not reduced the colony formation any more (Fig. 6B, C). In scramble-shRNA-expressing PCSC, vardenafil ranging from 0 μM to 100 μM dose-dependently and robustly reduced the mRNA expression of *fam65b* and vardenafil at 100 μM reduced the *fam65b* mRNA levels by 60%, however, in TAZ-shRNA-expressing PCSC, vardenafil only at 100 μM appeared to reduce the *fam65b* mRNA levels by 35% (Fig. 6D). Similarly, in scramble-shRNA-expressing PCSC, vardenafil ranging from 0 μM to 100 μM dose-dependently and robustly induced the mRNA expression of *cd24* and vardenafil at 100 μM increased the *cd24* mRNA levels by 5.0-fold, however, in TAZ-shRNA-expressing PCSC, though TAZ shRNA increased *cd24* mRNA levels by 4.8-fold, vardenafil only at 100 μM appeared to induce the *cd24* mRNA levels by 0.33-fold (Fig. 6E). Finally, in DDP-induced cytotoxicity to PCSC, vardenafil at 50 μM increased DDP-induced cytotoxicity by 2.5-fold in scramble-shRNA-expressing PCSC and TAZ knockdown increased DDP-induced cytotoxicity by 1.2-fold in TAZ-shRNA-expressing PCSC, however, vardenafil at 50 μM did not affected DDP-induced cytotoxicity any more in TAZ-shRNA-expressing PCSC (Fig. 6F). Thus, these data suggest that PDE5/cGMP/PKG signaling module maintain stemness of PCSC through Hippo/TAZ pathway.

PDE5/cGMP/PKG signal targeting to Hippo/TAZ pathway in maintaining stemness of PCSC xenografts

To test the roles of PDE5/cGMP/PKG and Hippo/TAZ signals in stemness *in vivo*, we next knocked down the expression of TAZ by TAZ-shRNA-expressing lentiviruses and inhibited PDE5 activity by oral administration of vardenafil at 40 mg/kg/d in PC3 cell and PCSC xenografts-bearing nude mice. The volumes of PC3 cell and PCSC xenografts with various treatments were time-dependently increased within 40-d post inoculation (Fig. 7A, Fig. S2A), though

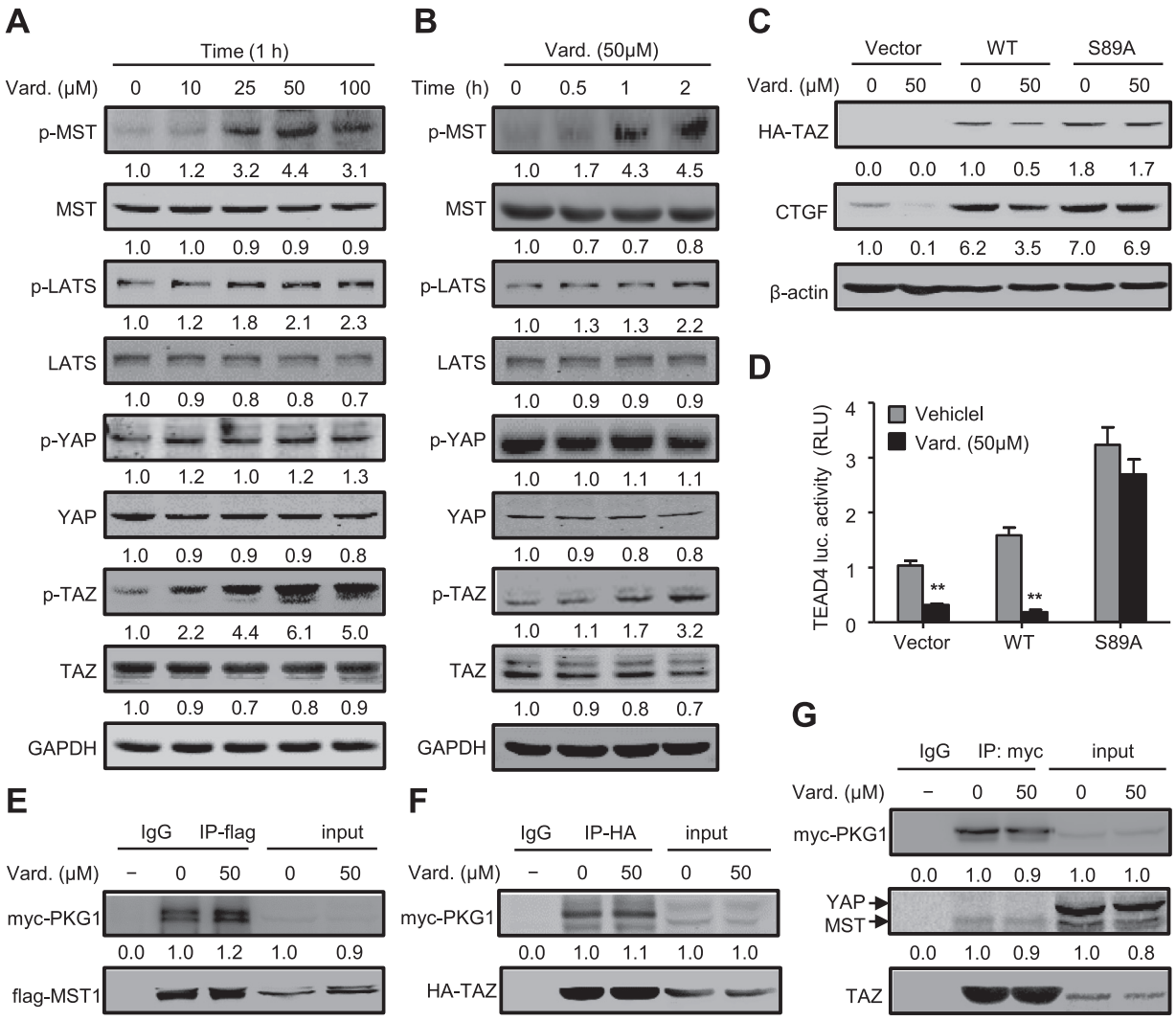

Fig. 5. PDE5/cGMP/PKG signal targets to Hippo pathway. (A) Immunoblot assays for the indicated proteins in PC3 cell treated with indicated concentrations of vardenafil for 1 hour. (B) Immunoblot assays for the indicated proteins in PC3 cell treated with 50 μM vardenafil for indicated times. (C) PC3 cells were transfected with empty vector, wild type TAZ (WT) or TAZ mutant and further treated with or without vardenafil for 12 hours. Immunoblot assays for indicated protein were performed. (D) TEAD4 luciferase activity in PC3 cells co-transfected with empty vector, wild type TAZ and its mutant, luciferase assays were performed 48 hours after transfection. (E) PC3 cells were co-transfected with myc-tagged PKG1 and flag-tagged MST1 for 48 hours, and treated with or without vardenafil at 50 μM for 1 hour, the cell lysates were subjected to immunoprecipitation by using flag antibody and the input samples were immunoblotted with the indicated antibodies. (F) PC3 cells were co-transfected with myc-tagged PKG1 and HA-tagged TAZ for 48 hours and treated with or without vardenafil for a further 1 hour, the cell lysates were subjected to immunoprecipitation by using HA antibody and the input samples were immunoblotted with the indicated antibodies. (G) PC3 cells were transfected with myc-tagged PKG1 for 48 hours and treated with or without vardenafil for a further 1 hour, the cell lysates were subjected to immunoprecipitation by using myc antibody and the input samples were immunoblotted with the indicated antibodies.

no significant difference appeared between the body weights of mice bearing the different xenografts (data not shown). From day 20, the volumes of scramble-shRNA-expressing and vehicle-treated xenografts were significantly higher than those of either TAZ-shRNA-expressing or vardenafil-treated xenografts, though from day 30, the volume of TAZ-shRNA-expressing and vardenafil-treated xenografts were significantly higher than those of TAZ-shRNA-expressing and vehicle-treated xenografts (Fig. 7A). Similar but less severe changes were also observed in PC3 cells (Fig. S2A, B). In day-40 PCSC xenografts, the volume of scramble-shRNA-expressing and vehicle-treated xenografts were 25%, 670%, and 192% higher than those of scramble-shRNA-expressing and vardenafil-treated xenografts, TAZ-shRNA-expressing and vehicle-treated xenografts, and TAZ-shRNA-expressing and vardenafil-treated xenografts, respectively (Fig. 7A, B).

To investigate the proliferation and apoptosis in PCSC and PC3 cell xenografts 40-d post inoculation, we further performed TUNEL and ki67 staining. In PCSC xenografts, vardenafil treatment led to significant increases in apoptosis but decreases in proliferation as compared with vehicle treatment, and TAZ shRNA resulted in robust increases in apoptosis and moderate decreases in proliferation as compared with scramble shRNA (Fig. 7C, D). Expectedly, the combination of TAZ shRNA and vardenafil treatment led to significantly less proliferation than TAZ shRNA alone, and unexpectedly, the combination of TAZ shRNA and vardenafil treatment resulted in significantly less apoptosis than TAZ shRNA alone (Fig. 7C, D). As a result, the Ki67/TUNEL index in scramble-shRNA-expressing and vardenafil-treated PCSC xenografts was approximately 9.0-fold less than those in scramble-shRNA-expressing and vehicle-treated PCSC xenografts, whereas the Ki67/TUNEL index in TAZ-shRNA-expressing and vehicle-treated PCSC xenografts was almost same as that in TAZ-shRNA-expressing and vardenafil-treated PCSC xenografts (Fig. 7E). Likewise, in PC3 cells, vardenafil treatment led to significant increases in apoptosis but slight decreases in proliferation as compared with vehicle treatment, and

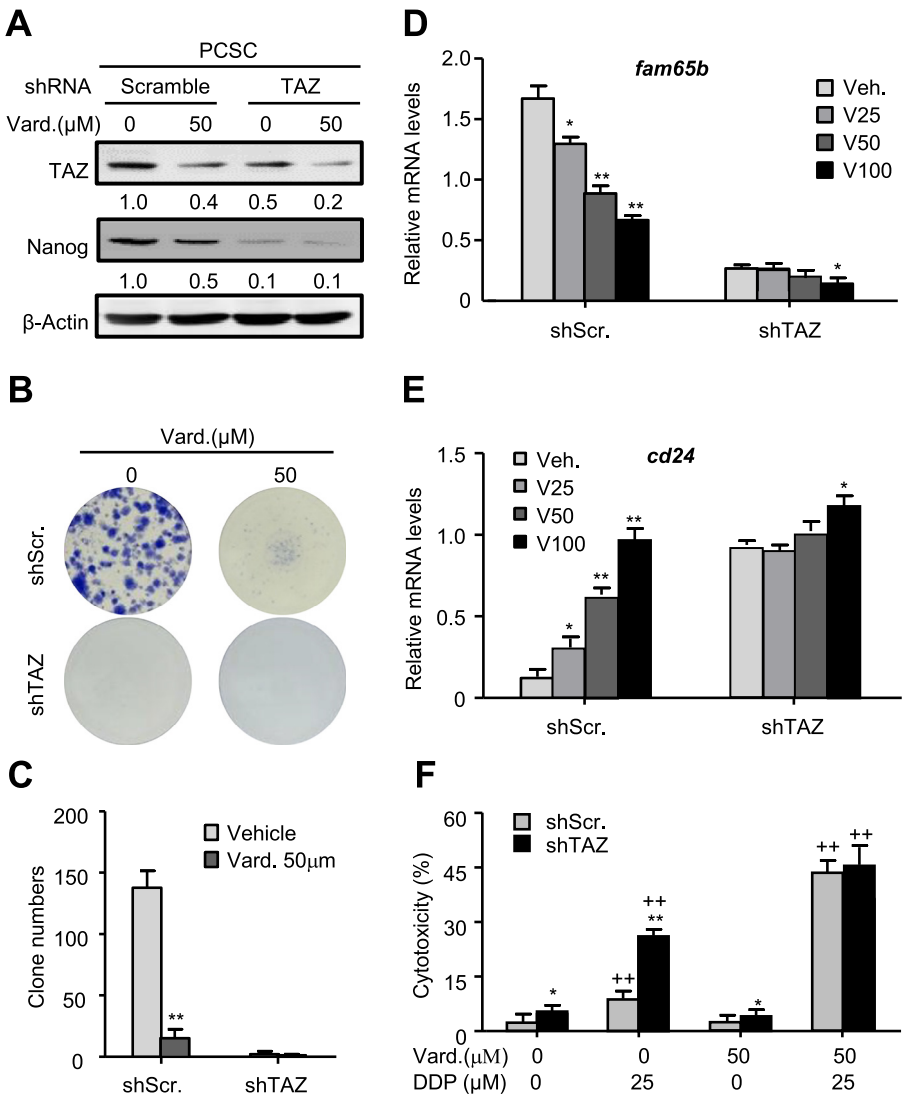

Fig. 6. Inhibition of PDE5 reduces stemness of PCSC through TAZ. (A) TAZ and Nanog protein levels in PCSC expressing scramble- or TAZ-shRNA in the presence or absence of vardenafil at 50 μM. (B, C) Colony formation assays and quantification in PCSC expressing scramble- or TAZ-shRNA in the presence or absence of vardenafil at 50 μM. (D, E) Messenger mRNA levels of *fam65b* and *cd24* in PCSC expressing scramble- or TAZ-shRNA in the presence or absence of vardenafil at indicated concentrations. (F) Cytotoxicity of DDP to PCSC expressing scramble- or TAZ-shRNA in the presence or absence of vardenafil at 50 μM. $^{*}p < 0.05$, $^{**}p < 0.01$ versus vehicle treated and scramble-shRNA-expressing cells, $^{++}p < 0.01$ versus scramble-shRNA expressing cells.

TAZ shRNA resulted in robust increases in apoptosis and significant increases in proliferation as compared with scramble shRNA (Fig. S2C, D). However, the combination of TAZ shRNA and vardenafil treatment led to no significant difference in proliferation as compared with TAZ shRNA alone, and the combination of TAZ shRNA and vardenafil treatment resulted in moderately less apoptosis than TAZ shRNA alone (Fig. 7C, D). As a result, the Ki67/TUNEL index in scramble-shRNA-expressing and vardenafil-treated PCSC xenografts was approximately 3.0-fold less than those in scramble-shRNA-expressing and vehicle-treated PC3 cell xenografts, whereas the Ki67/TUNEL index in TAZ-shRNA-expressing and vehicle-treated PC3 cell xenografts was slightly less than that in TAZ-shRNA-expressing and vardenafil-treated PC3 cell xenografts (Fig. S2E).

Vardenafil treatment decreased the *fam65b* mRNA levels by 70% in PCSC xenografts and 75% in PC3 cell xenografts and induced *cd24* and *lcp1* mRNA levels by 100% and 650% in PCSC xenografts and 125% and 435% in PC3 cell xenografts, while TAZ shRNA reduced the mRNA levels of *fam65b* by 73% in PCSC xenografts and 72% in PC3 cell xenografts, and induced *cd24* and *lcp1* mRNA levels by 105% and 655% in PCSC xenografts and 120% and 228% in PC3 cell xenografts (Fig. 7F, Fig. S2F). Vardenafil treatment in TAZ-shRNA-expressing PCSC xenografts did not affect these mRNA levels any more, whereas vardenafil treatment in TAZ-shRNA-expressing PC3 cell xenografts significantly decreased *fam65b* mRNA levels by 80% but increased *cd24* and *lcp1* mRNA levels by 2.8- and 8.6-fold, respectively (Fig. 7F, Fig. S2F). In addition, vardenafil treatment decreased the Nanog, Sox2 and TAZ protein levels by 70%, 90%, and 90%, respectively, while TAZ knockdown in PCSC xenografts reduced the Nanog, Sox2 and TAZ protein levels by 80%, 80%, and 70%, respectively. However, neither vardenafil treatment nor TAZ knockdown affected the protein levels of YAP. Importantly, in TAZ-shRNA-expressing PCSC xenografts, vardenafil treatment did not significantly affect the Nanog and Sox2 protein levels any more (Fig. 7G). Likewise, vardenafil treatment decreased the *ctgf* and *cyr61* mRNA levels by 59% and 60%, respectively, while TAZ knockdown reduced the *ctgf* and *cyr61* mRNA levels by 60% and 75%, respectively. Importantly, in TAZ-shRNA-expressing PCSC, vardenafil treatment did not significantly affect the *ctgf* and *cyr61* mRNA levels any more (Fig. 7H). Thus, PDE5/cGMP/PKG signal targets to Hippo/TAZ pathway in maintaining stemness in PCSC xenografts.

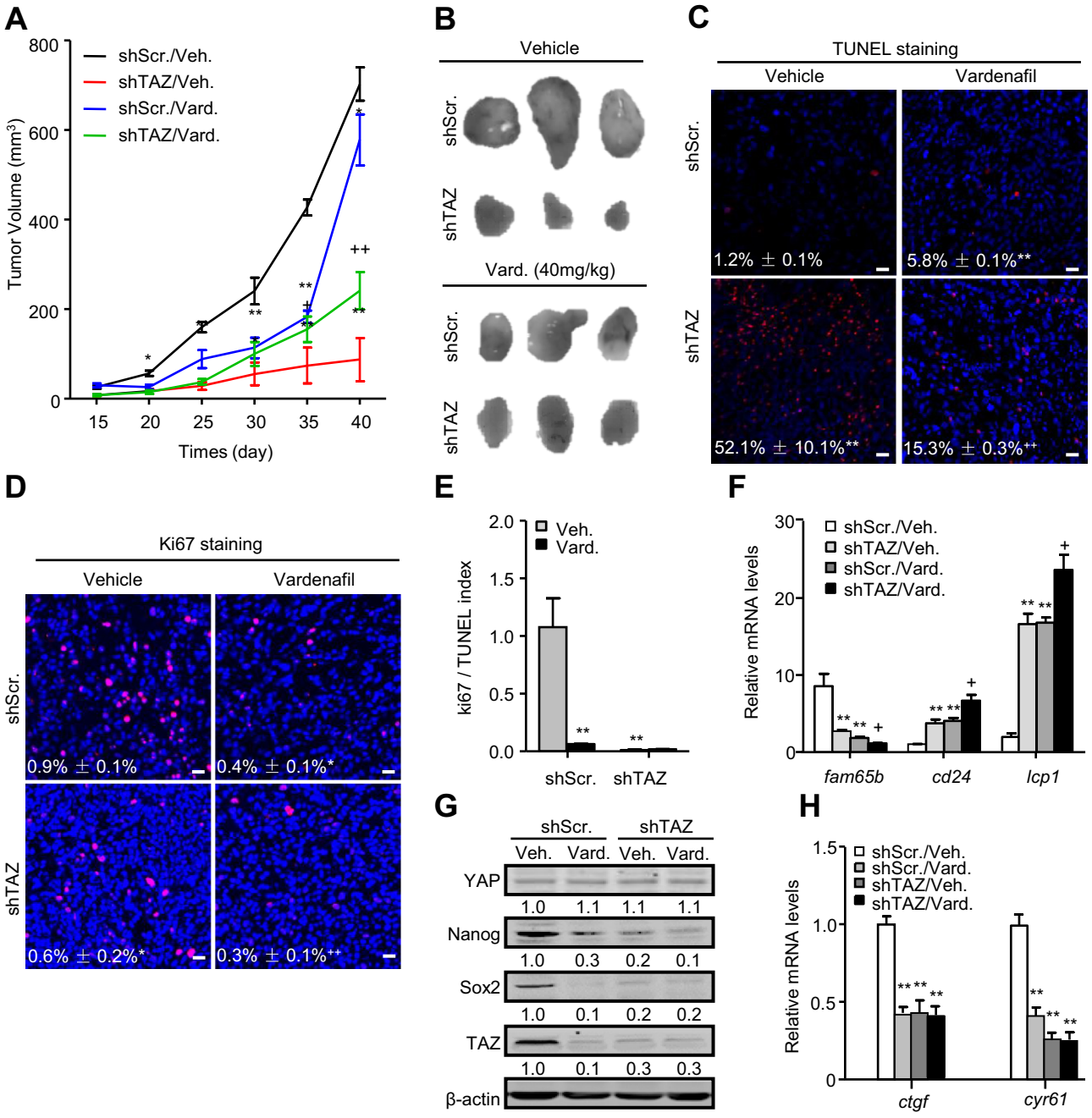

Fig. 7. Inhibition of PDE5 decreases stemness of PCSC *in vivo*. (A) Volumes of xenografts expressing scramble- or TAZ-shRNA and treated with or without vardenafil for indicated times. (B) Images of the representative xenografts on day 40. (C) TUNEL staining for the xenografts on day 40. (D) ki67 staining for the xenografts on day 40. (E) ki67/tunel index = ki67 positive cells numbers ÷ apoptosis positive cells numbers. (F) Quantitative RT-PCR assays for *fam65b*, *cd24* and *lcp1* in xenografts expressing scramble- or TAZ-shRNA and treated with or without vardenafil for 25 days. (G) Immunoblot assays for TAZ, Nanog and SOX2 expression in xenografts expressing scramble- or TAZ-shRNA and treated with or without vardenafil for 25 days. (H) Quantitative RT-PCR assays for *ctgf* and *cyr61* in xenografts expressing scramble- or TAZ-shRNA and treated with or without vardenafil for 25 days. $^{*}p < 0.05$, $^{**}p < 0.01$ versus vehicle-treated and scramble-shRNA-expressing xenografts; $^{+}p < 0.05$, $^{++}p < 0.01$ versus TAZ-shRNA expressing and vehicle-treated xenografts.

Discussion

By *in vitro* cell culture and *in vivo* xenograft approaches, we have uncovered that PDE/cGMP/PKG signal targets to Hippo/TAZ pathway in maintaining stemness of prostate cancer stem cells. In this molecular event, inhibition of PDE5 activity by its inhibitor or endogenous NO in PCSC results in elevation of cGMP and activation of cGMP-dependent PKG, which in turn activates MST/LATS and thereby destabilizes TAZ in cytosol, resulting in attenuation of TAZ-mediated gene transcription and consequent reduction of stemness in prostate cancer stem cells (Fig. 8).

CSC making up 1~5% of most tumors are common subsets within a variety of malignancies, whereas in PC3 cells, an androgen receptor–negative and undifferentiated human prostate cancer cell line, the proportion almost reaches 10% [1]. Thus, PC3 cell is an ideal *in vitro* model for PCSC biological study. By limiting dilution approach, we have succeeded in isolating PC3 cells-derived PCSC. In PCSC, higher mRNA levels of *fam65b* and lower mRNA levels of *cdc42*

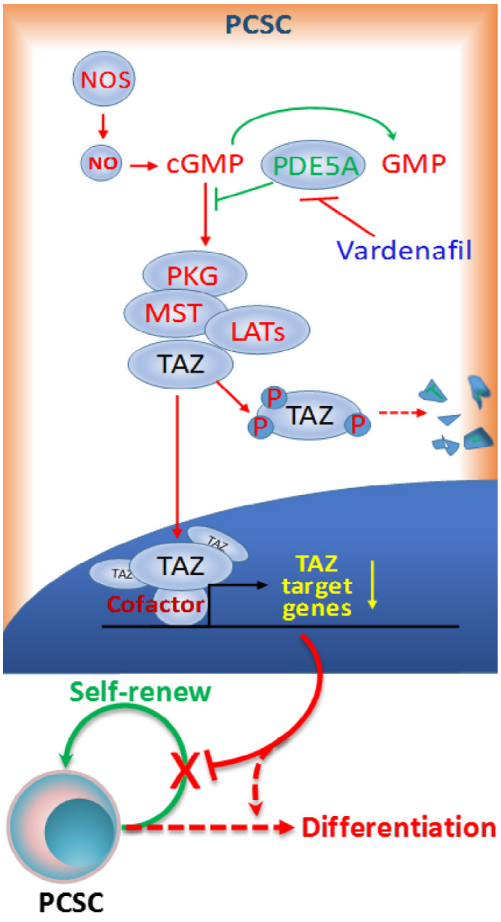

Fig. 8. Schematic diagram underlying the Hippo/TAZ-dependent maintenance of stemness in prostate cancer stem cells by PDE5/cGMP/PKG signal. Inhibition of PDE5 by its inhibitors, vardenafil, or endogenous NO results in elevation of cGMP and activation of cGMP-dependent protein kinase, which further activates MST and thereby destabilizes TAZ in cytosol, leading to attenuation of TAZ-mediated gene transcription and the consequent reduction of stemness in prostate cancer stem cells.

and *lcp1* than in PC3 cells attest the notion that *fam65b*^{high}/*cd24*^{low}/*lcp1*^{low} serves as effective PCSC markers [2]. Higher expression of Nanog and Sox2 in PCSC than in PC3 and more chemoresistance in PCSC than in PC3 cells further confirm that our obtained PCSC possess the stemness, quiescence, and potentiality to self-renew characterizing cancer stem cells. YAP and TAZ are the cores to Hippo signaling pathway. In prostate cancer, YAP is aberrantly elevated and serves as an oncogene [14,15]. Besides, 14-3-3σ, a suppressor involved in cytoplasmic retention of TAZ and YAP is frequently methylated in prostate carcinoma patient's tissues and cancer cell lines, resulting in its gene silence [31]. In the present study, we have found that TAZ but not YAP is dramatically elevated in PCSC, which contributes to maintaining stemness of PCSC. Consistent with our findings, previous studues have reported that TAZ but not YAP confers the stem cell characteristics in breast cancer stem cells and oral cancer [12,32]. On the country, YAP but not TAZ confers the stem cell characteristics in hepatocellular carcinoma and gastric cancer [13,33].

NOS is the enzyme responsible for producing NO and NO activates soluble guanylyl cyclases to increase the intracellular cGMP levels and activate PKG [34]. Alternatively, inhibition of PDE5 by its specific inhibitors decreases the degradation of intracellular cGMP levels and subsequently activates PKG [35]. We have found that the main components of NO (PDE5)/cGMP/PKG signaling pathways are widely expressed in prostate cancer cells, and that PC3 cells with high NO levels express less TAZ than PC3 cells with low NO levels. This finding prompts us to speculate the possible roles of NO (PDE5)/cGMP/PKG signal in PCSC. Though several previous studies have hinted at the possible roles of NO/cGMP/PKG signaling module in differentiation of stem cell and stemness of cancer stem cells, its downstream signaling events remain largely elusive [20,36]. In the present study, we have shown that activation of cGMP/PKG signaling by PDE5 inhibitor reduces TAZ-mediated maintenance of stemness in PCSC; this finding conflicts previous studies showing that NO induces cancer stem-like phenotype and that increased NOS2 predicts poor survival in estrogen receptor-negative breast cancer patients [37,38]. We suggest that either elevation of NO or activation of cGMP/PKG signaling by inhibition of PDE5 could play diverse roles in tumor biological behavior.

Despite the fact that PKG co-exists in one immunocomplex with MST and PKG indeed phosphorylates MST, we still do not know whether PKG phosphorylates MST directly or indirectly. Further *in vitro* and *in vivo* phosphorylation assays are worthy of investigation. In addition, activation of MST by PKG in turn activates LATS and subsequently phophorylates TAZ at Serine89, whereas activated LATS neither affects the YAP phosphorylation nor the intracellular YAP protein levels. It is likely that phosphorylation of YAP is LATS1/2-independent in our experimental system. This notion has been supported by the following evidence: the metabolic mevalonate/cholesterol pathway raises YAP Serine127 phosphorylation in a LATS1/2-independent manner; fractionation of liver extracts reveal that fractions void of LATS1/2 are still able to phosphorylate YAP at Serine127; in keratinocytes, β-catenin works in concert with an unknown kinase to sustain YAP phosphorylation at Serin127 [39–42]. Nuclear TAZ inhibits apoptosis and promotes proliferation, while cGMP/PKG signal reduces cell growth and induces apoptosis in a variety of tumor tissues and cells [43–46]. Consistently, our data show that TAZ knockdown robustly induces cell apoptosis but moderately decreases cell proliferation in PCSC xenografts, and that vardenafil robustly reduces cell proliferation and significantly induces apoptosis. However, a combination of TAZ knockdown and vardenafil treatment in PCSC xenografts leads to significantly less apoptosis than TAZ knockdown alone, which accounts for the unexpected changes in outgrowth of PCSC xenografts. We suggest that the trans-differential effects of either TAZ knockdown or vardenafil treatment should be responsible for the observed less apoptosis in PCSC xenografts with TAZ knockdown and vardenafil treatment than in PCSC xenografts with TAZ knockdown and vehicle treatment. This notion is supported by our findings showing that either TAZ knockdown or vardenafil treatment leads to less apoptosis in PC3 cell xenografts than in PCSC xenografts.

Because its elevation occurs with increasing tumor grade and stage, PDE5 has been suggested to be involved in tumor progression, and PDE5 selective inhibitors has been suggested to serve as a potent anticancer drugs by promoting the cell apoptosis and suppressing the cell proliferation [26,43,44,47,48]. Most importantly, we further have demonstrated that vardenafil through activation of Hippo/TAZ pathway robustly potentiates the sensitivity of PCSC to chemotherapy *in vitro*, though *in vivo* experiments are essential for further confirmation. Consistent with our finding, previous studies have suggested that PDE5 inhibitors enhance the chemotherapeutic efficacy of anticancer drugs in prostate and other cancers. Sulindac sulfide and exisulind suppress outgrowth and promote apoptosis in both androgen-sensitive (LNCaP) and androgen-insensitive (PC3) prostate cancer cells [48,49]. Exisulind also inhibits the outgrowth of prostate cancer cells in an athymic nude mouse xenograft model [50]. At a low dose, exisulind in combination with colecoxib, a cyclooxygenase-2 (Cox-2) inhibitor, prevents prostate carcinogenesis and enhances apoptosis [51]. A recent study has demonstrated that sildenafil interacts greater than additive fashion

with celecoxib to kill multiple tumor cell types including human glioma cells as well as their associated activated microglia [52]. Therefore, a combination of PDE5 specific inhibitors could be very efficacious against prostate cancer initiation, metastasis, relapse and chemoresistance by activation of Hippo/TAZ pathway and attenuating stemness of prostate cancer cells.

Funding

This project was supported by National Natural Science Foundation of China (No. 31571493, No. 31271561, No. 31071292, No. 81370713, No. 81071751), 973 Program (No. 2011CB944403), Natural Science Foundation of Zhejiang Province (LY13H160020), and Foundation of Science Technology Department of Zhejiang Province (No. 2014C33183).

Acknowledgments

Flag-tagged MST and TEAD luciferase reporter plasmids were gifted from Dr. Bin Zhao (Zhejiang University).

Conflict of interest

The authors declare no conflict of interest for this work.

Appendix: Supplementary material

Supplementary data to this article can be found online at doi:10.1016/j.canlet.2016.05.010.

References

[1] H. Li, X. Chen, T. Calhoun-Davis, K. Claypool, D.G. Tang, PC3 human prostate carcinoma cell holoclones contain self-renewing tumor-initiating cells, Cancer Res. 68 (2008) 1820–1825.
[2] K. Zhang, D.J. Waxman, PC3 prostate tumor-initiating cells with molecular profile *FAM65B*high/*MFI2*low/*LEF1*low increase tumor angiogenesis, Mol. Cancer 9 (2010) 319–332.
[3] A.M. De Marzo, W.G. Nelson, A.K. Meeker, D.S. Coffey, Stem cell features of benign and malignant prostate epithelial cells, J. Urol. 160 (1998) 2381–2392.
[4] M.M. Shen, C. Abate-Shen, Molecular genetics of prostate cancer: new prospects for old challenges, Genes Dev. 24 (2010) 1967–2000.
[5] C. Liu, K. Kelnar, B. Liu, X. Chen, T. Calhoun-Davis, D.G. Tang, et al., The microRNA miR-34a inhibits prostate cancer stem cells and metastasis by directly repressing CD44, Nat. Med. 17 (2011) 211–215.
[6] B. Zhao, L. Li, K.L. Guan, Hippo signaling at a glance, J. Cell Sci. 123 (2010) 4001–4006.
[7] S. Piccolo, S. Dupont, M. Cordenonsi, The biology of YAP/TAZ: hippo signaling and beyond, Physiol. Rev. 94 (2014) 1287–1312.
[8] J. Dong, G. Feldmann, J. Huang, S. Wu, N. Zhang, D. Pan, et al., Elucidation of a universal size-control mechanism in Drosophila and mammals, Cell 130 (2007) 1120–1133.
[9] Q.Y. Lei, H. Zhang, B. Zhao, Z.Y. Zha, F. Bai, K.L. Guan, et al., TAZ promotes cell proliferation and epithelial-mesenchymal transition and is inhibited by the hippo pathway, Mol. Cell. Biol. 28 (2008) 2426–2436.
[10] M. Kim, T. Kim, R.L. Johnson, D.S. Lim, Transcriptional co-repressor function of the hippo pathway transducers YAP and TAZ, Cell Rep. 11 (2015) 270–282.
[11] B. Zhao, K. Tumaneng, K.L. Guan, The Hippo pathway in organ size control, tissue regeneration and stem cell self-renewal, Nat. Cell Biol. 13 (2011) 877–883.
[12] M. Cordenonsi, F. Zanconato, L. Azzolin, M. Forcato, A. Rosato, S. Piccolo, et al., The Hippo transducer TAZ confers cancer stem cell-related traits on breast cancer cells, Cell 147 (2011) 759–772.
[13] H. Hayashi, T. Higashi, N. Yokoyama, T. Kaida, K. Sakamoto, H. Baba, et al., An imbalance in TAZ and YAP expression in hepatocellular carcinoma confers cancer stem cell-like behaviors contributing to disease progression, Cancer Res. 75 (2015) 4985–4997.
[14] L.T. Nguyen, M.S. Tretiakova, M.R. Silvis, J. Lucas, O. Klezovitch, V. Vasioukhin, et al., ERG activates the YAP1 transcriptional program and induces the development of age-related prostate tumors, Cancer Cell 27 (2015) 797–808.
[15] L. Zhang, S. Yang, X. Chen, S. Stauffer, F. Yu, J. Dong, et al., The hippo pathway effector YAP regulates motility, invasion, and castration-resistant growth of prostate cancer cells, Mol. Cell. Biol. 35 (2015) 1350–1362.
[16] E. Butt, K. Abel, M. Krieger, D. Palm, V. Hoppe, U. Walter, et al., cAMP- and cGMP-dependent protein kinase phosphorylation sites of the focal adhesion vasodilator-stimulated phosphoprotein (VASP) in vitro and in intact human platelets, J. Biol. Chem. 269 (1994) 14509–14517.
[17] Y. Gong, C.Y. Xu, J.R. Wang, X.H. Hu, D. Hong, X.M. Wu, et al., Inhibition of phosphodiesterase 5 reduces bone mass by suppression of canonical Wnt signaling, Cell Death Dis. 5 (2014) doi:10.1038/cddis.2014.510.
[18] N. Marsh, A. Marsh, A short history of nitroglycerine and nitric oxide in pharmacology and physiology, Clin. Exp. Pharmacol. Physiol. 27 (2000) 313–319.
[19] E.C. Vasquez, A.L. Gava, J.B. Graceli, C.M. Balarini, B.P. Campagnaro, S.S. Meyrelles, et al., Novel Therapeutic Targets for Phosphodiesterase 5 Inhibitors: current state-of-the-art on systemic arterial hypertension and atherosclerosis, Curr. Pharm. Biotechnol. 17 (2015) doi:10.2174/1389201017666151223123904.
[20] J.S. Krumenacker, S. Katsuki, A. Kots, F. Murad, Differential expression of genes involved in cGMP-dependent nitric oxide signaling in murine embryonic stem (ES) cells and ES cell-derived cardiomyocytes, Nitric Oxide 14 (2006) 1–11.
[21] L.P. D'Atri, E. Malaver, M.A. Romaniuk, R.G. Pozner, S. Negrotto, M. Schattner, Nitric oxide: news from stem cells to platelets, Curr. Med. Chem. 16 (2009) 417–429.
[22] N. Ybarra, J.R. del Castillo, E. Troncy, Involvement of the nitric oxide-soluble guanylyl cyclase pathway in the oxytocin-mediated differentiation of porcine bone marrow stem cells into cardiomyocytes, Nitric Oxide 24 (2011) 25–33.
[23] N.N. Hoke, F.N. Salloum, D.A. Kass, A. Das, R.C. Kukreja, Preconditioning by phosphodiesterase-5 inhibition improves therapeutic efficacy of adipose-derived stem cells following myocardial infarction in mice, Stem Cells 30 (2012) 326–335.
[24] I. Barone, S. Catalano, A. Campana, C. Giordano, B. Gyorffy, S. Ando, et al., Expression and function of phosphodiesterase type 5 in human breast cancer cell lines and tissues: implications for targeted therapy, Clin. Cancer Res. (2015) doi:10.1158/1078-0432.CCR-15-1900.
[25] N. Li, X. Chen, B. Zhu, V. Ramírez-Alcántara, J.C. Canzoneri, G.A. Piazza, et al., Suppression of β-catenin/TCF transcriptional activity and colon tumor cell growth by dual inhibition of PDE5 and 10, Oncotarget 6 (2015) 27403–27415.
[26] F. Karami-Tehrani, M. Moeinifard, M. Aghaei, M. Atri, Evaluation of PDE5 and PDE9 expression in benign and malignant breast tumors, Arch. Med. Res. 43 (2012) 470–475.
[27] Z. Shi, A.K. Tiwari, S. Shukla, R.W. Robey, S. Singh, Z.S. Chen, et al., Sildenafil reverses ABCB1- and ABCG2-mediated chemotherapeutic drug resistance, Cancer Res. 71 (2011) 3029–3041.
[28] J.L. Roberts, L. Booth, A. Conley, N. Cruickshanks, M. Malkin, P. Dent, et al., PDE5 inhibitors enhance the lethality of standard of care chemotherapy in pediatric CNS tumor cells, Cancer Biol. Ther. 15 (2014) 758–767.
[29] L. Chen, H. Zhu, Y. Pan, C. Tang, M. Watanabe, X. Wu, et al., Ascorbic acid uptaken by sodium-dependent vitamin C transporter 2 induces βhCG expression through Sp1 and TFAP2A transcription factors in human choriocarcinoma cells, J. Clin. Endocrinol. Metab. 97 (2012) 1667–1676.
[30] M. Niyazi, I. Niyazi, C. Belka, Counting colonies of clonogenic assays by using densitometric software, Radiat. Oncol. 2 (2007) 4–7.
[31] R. Henrique, C. Jerónimo, M.O. Hoque, A.L. Carvalho, J. Oliveira, D. Sidransky, et al., Frequent 14-3-3 sigma promoter methylation in benign and malignant prostate lesions, DNA Cell Biol. 24 (2005) 264–269.
[32] Z. Li, Y. Wang, Y. Zhu, C. Yuan, D. Wang, J. Cheng, et al., The Hippo transducer TAZ promotes epithelial to mesenchymal transition and cancer stem cell maintenance in oral cancer, Mol. Oncol. 9 (2015) 1091–1105.
[33] D. Fujimoto, Y. Ueda, Y. Hirono, T. Goi, A. Yamaguchi, PAR1 participates in the ability of multidrug resistance and tumorigenesis by controlling Hippo-YAP pathway, Oncotarget 6 (2015) 34788–34799.
[34] K.S. Madhusoodanan, F. Murad, NO-cGMP signaling and regenerative medicine involving stem cells, Neurochem. Res. 32 (2007) 681–694.
[35] Y.H. Jeon, Y.S. Heo, C.M. Kim, Y.L. Hyun, T.G. Lee, J. Cho, et al., MPhosphodiesterase: overview of protein structures, potential therapeutic applications and recent progress in drug development, Cell. Mol. Life Sci. 62 (2005) 1198–1220.
[36] K. Mujoo, V.G. Sharin, N.S. Bryan, J.S. Krumenacker, C. Sloan, F. Murad, et al., Role of nitric oxide signaling components in differentiation of embryonic stem cells into myocardial cells, Proc. Natl. Acad. Sci. U.S.A. 105 (2008) 18924–18929.
[37] J. Firger, Nitric oxide inhibitors hit target for triple-negative breast cancer, J. Natl. Cancer Inst. 107 (2015) doi:10.1093/jnci/djv235.
[38] M.A. Puglisi, C. Cenciarelli, V. Tesori, M. Cappellari, M. Martini, A. Gasbarrini, et al., High nitric oxide production, secondary to inducible nitric oxide synthase expression, is essential for regulation of the tumour-initiating properties of colon cancer stem cells, J. Pathol. 236 (2015) 479–490.
[39] S. Basu, N.F. Totty, M.S. Irwin, M. Sudol, J. Downward, Akt phosphorylates the Yes-associated protein, YAP, to induce interaction with 14-3-3 and attenuation of p73-mediated apoptosis, Mol. Cell 11 (2003) 11–23.
[40] D. Zhou, C. Conrad, F. Xia, J.S. Park, B. Payer, N. Bardeesy, et al., Mst1 and Mst2 maintain hepatocyte quiescence and suppress hepatocellular carcinoma development through inactivation of the Yap1 oncogene, Cancer Cell 16 (2009) 425–438.
[41] K. Schlegelmilch, M. Mohseni, O. Kirak, J. Pruszak, J.R. Rodriguez, F.D. Camargo, et al., Yap1 acts downstream of alpha-catenin to control epidermal proliferation, Cell 144 (2011) 782–795.
[42] G. Sorrentino, N. Ruggeri, V. Specchia, M. Cordenonsi, M. Mano, G. Del Sal, et al., Metabolic control of YAP and TAZ by the mevalonate pathway, Nat. Cell Biol. 16 (2014) 357–366.

[43] M. Sarfati, V. Mateo, S. Baudet, M. Rubio, C. Fernandez, H. Merle-Beral, et al., Sildenafil and vardenafil, types 5 and 6 phosphodiesterase inhibitors, induce caspase-dependent apoptosis of B-chronic lymphocytic leukemia cells, Blood 101 (2003) 265–269.
[44] B. Zhu, L. Vemavarapu, W.J. Thompson, S.J. Strada, Suppression of cyclic GMP-specific phosphodiesterase 5 promotes apoptosis and inhibits growth in HT29 cells, J. Cell. Biochem. 94 (2005) 336–350.
[45] M. Wang, Y. Liu, J. Zou, R. Yang, F. Xuan, H. Cui, et al., Transcriptional co-activator TAZ sustains proliferation and tumorigenicity of neuroblastoma by targeting CTGF and PDGF-beta, Oncotarget 6 (2015) 9517–9530.
[46] H. Xiao, N. Jiang, B. Zhou, Q. Liu, C. Du, TAZ regulates cell proliferation and epithelial-mesenchymal transition of human hepatocellular carcinoma, Cancer Sci. 106 (2015) 151–159.
[47] L. Liu, T. Underwood, H. Li, R. Pamukcu, W.J. Thompson, Specific cGMP binding by the cGMP binding domains of cGMP-binding cGMP specific phosphodiesterase, Cell. Signal. 14 (2002) 45–51.
[48] J.T. Lim, G.A. Piazza, R. Pamukcu, W.J. Thompson, I.B. Weinstein, Exisulind and related compounds inhibit expression and function of the androgen receptor in human prostate cancer cells, Clin. Cancer Res. 9 (2003) 4972–4982.
[49] J.T. Lim, G.A. Piazza, E.K. Han, T.M. Delohery, H. Li, I.B. Weinstein, et al., Sulindac derivatives inhibit growth and induce apoptosis in human prostate cancer cell lines, Biochem. Pharmacol. 58 (1999) 1097–1107.
[50] E.T. Goluboff, A. Shabsigh, J.A. Saidi, I.B. Weinstein, N. Mitra, C.A. Olsson, et al., Exisulind (sulindac sulfone) suppresses growth of human prostate cancer in a nude mouse xenograft model by increasing apoptosis, Urology 53 (1999) 440–445.
[51] B.A. Narayanan, B.S. Reddy, M.C. Bosland, D. Nargi, L. Horton, N.K. Narayanan, et al., Exisulind in combination with celecoxib modulates epidermal growth factor receptor, cyclooxygenase-2, and cyclin D1 against prostate carcinogenesis: in vivo evidence, Clin. Cancer Res. 13 (2007) 5965–5973.
[52] L. Booth, J.L. Roberts, N. Cruickshanks, S. Tavallai, T. Webb, P. Dent, et al., PDE5 inhibitors enhance celecoxib killing in multiple tumor types, J. Cell. Physiol. 230 (2015) 1115–1127.